EFFECTS OF LONGITUDINAL AND TRANSVERSE RESISTIVE-WALL WAKEFIELDS ON ERLS

N. Nakamura#
Institute for Solid State Physics(ISSP), University of Tokyo
5-1-5 Kashiwanoha, Kashiwa, Chiba 277-8581, Japan.

Abstract

Exact expressions of longitudinal and transverse resistive-wall impedances for a round pipe with a finite thickness were analytically obtained to accurately evaluate effects of resistive-wall wakefields on energy recovery linacs(ERLs). Parasitic loss in an ERL vacuum chamber due to the longitudinal impedance was evaluated and found to be serious compared with 3rd generation SR sources because of the shorter bunch length. It was also shown by the calculation result of longitudinal resistive-wall impedance of a two-layer round pipe that copper coating is effective for reducing the parasitic loss of a stainless steel(SS) chamber. Transverse resistive-wall wake functions of round pipes were numerically calculated using the exact impedance expression to simulate transverse multi-bunch beam motions due to resistive-wall wakefields in ERLs. Possibility of resistive-wall beam breakup(BBU) in the compact ERL and in a long undulator chamber of a 5-GeV ERL was discussed based on simulation results.

INTRODUCTION

In ERL-based synchrotron radiation(SR) sources, high-current and short-bunch beams are circulated. Such a beam can generate strong wakefields in resistive-wall ERL components and the wakefields seriously affect the components and the beam itself. Transverse multi-bunch beam breakup due to the resistive-wall wake was already studied with analytical and simulation approaches using the conventional expression of the resistive-wall wake function[1][2]. Although the study results implied that the beam position displacement due to the resistive-wall wake infinitely increases with time, it was also pointed out that the conventional expression of the resistive-wall wake function is valid only in a limited time range[2]. In this paper, exact expressions of the longitudinal and transverse impedances are derived to correctly estimate the resistive-wall impedances and their effects on ERLs. Transverse multi-bunch beam motions are simulated with the exact wake functions. Furthermore parasitic loss in a vacuum chamber due to the longitudinal resistive-wall wakefields is also evaluated.

EXACT EXPRESSIONS FOR RESISTIVE-WALL IMPEDANCES

Longitudinal Impedance

An exact expression of the longitudinal resistive-wall impedance (per unit length) of a round pipe with an inner radius b and a thickness d was analytically derived as follows:

$$Z_{//}(\omega)=\frac{-i}{2\pi\varepsilon_0 bc\left\{\left(\frac{\omega}{\lambda c}+\frac{\lambda c}{\omega}\right)\alpha_l-\frac{b\omega}{2c}\right\}} \quad (1)$$

$$\alpha_l=\frac{J_1(\lambda b)N_0(\lambda(b+d))-N_1(\lambda b)J_0(\lambda(b+d))}{J_0(\lambda b)N_0(\lambda(b+d))-N_0(\lambda b)J_0(\lambda(b+d))}$$

$$\lambda=\frac{i+sgn(\omega)}{\delta}\quad\left(\delta=\sqrt{\frac{2}{\sigma\mu_0|\omega|}}\right)$$

Here σ, ε_0, μ_0, c, i, ω, and δ are the electric conductivity of the pipe, the permittivity and permeability of vacuum, the velocity of light, the imaginary unit, the angular frequency and the skin depth of the pipe, and J_0, J_1, N_0 and N_1 are the 0th-order and 1st-order Bessel functions of the 1st and 2nd kinds, respectively. The permittivity and permeability of the pipe are assumed to be equal to or approximated by those of vacuum. The $sgn(\omega)$ means the sign of ω. If the pipe thickness becomes infinity, the expression is rewritten as Eq. (2) with the 0th-order and 1st-order Hankel functions of the 1st kind, $H_0^{(1)}$ and $H_1^{(1)}$.

$$Z_{//}(\omega)=\frac{-i}{2\pi\varepsilon_0 bc\left\{\left(\frac{\omega}{\lambda c}+\frac{\lambda c}{\omega}\right)\frac{H_1^{(1)}(\lambda b)}{H_0^{(1)}(\lambda b)}-\frac{b\omega}{2c}\right\}} \quad (2)$$

If one considers the frequency range satisfying the conditions of $|\lambda|b>>1$, $|\lambda|>>|\omega/c|$, $|\lambda|>>b\omega^2/c^2$, the conventional impedance expression of Eq. (3) is derived from Eq. (2).

$$Z_{//}(\omega)=\frac{\omega Z_0\delta}{4\pi bc}\{sgn(\omega)-i\}\quad\left(Z_0=\sqrt{\frac{\mu_0}{\varepsilon_0}}\right) \quad (3)$$

Here Z_0 is the impedance of vacuum.

Figure 1 shows the real parts of the resistive-wall impedances of stainless steel(SS) pipes with b=8 mm and σ=1.4×10^6 Ω^{-1}m^{-1} calculated from Eqs. (1) and (2). For comparison, the conventional expression of Eq. (3) is shown in the figure. The real parts of the exact impedances have two kinds of cut-offs, low and high frequency cut-offs. The high-frequency cut-off depends on only the pipe radius. On the other hand, the low-frequency cut-off depends on both pipe radius and thickness. Only in the intermediate frequency range, the impedances are approximated by Eq. (3) as shown in Fig. 1.

#nakamura@issp.u-tokyo.ac.jp

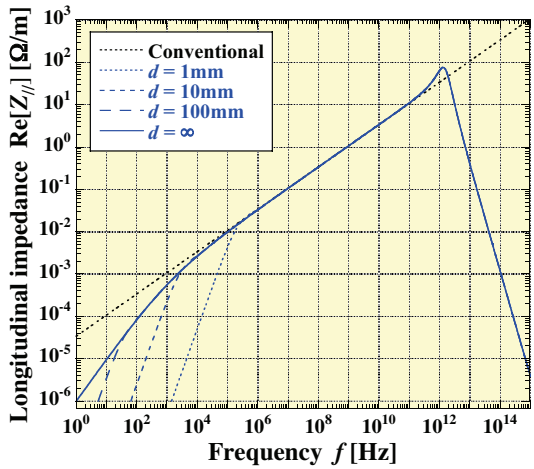

Figure 1: Longitudinal resistive-wall impedances of round pipes with an inner radius of 8 mm and thicknesses of 1, 10, 100 mm and infinity. The conventional impedance expression is also plotted by a black dotted line.

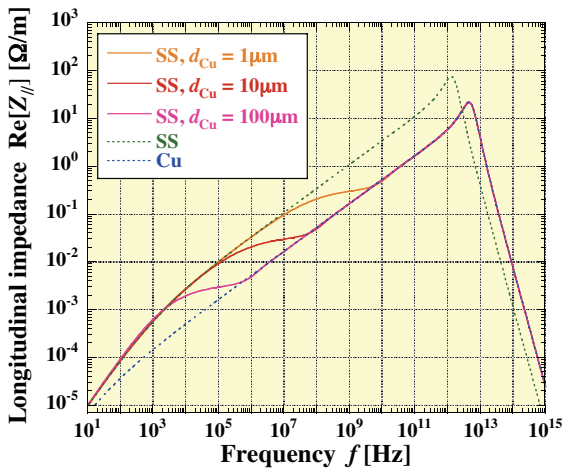

Figure 2: Longitudinal resistive-wall impedances of Cu-coated stainless steel(SS) pipes with an inner radius of 8 mm and Cu-coating thicknesses of 1, 10, 100 μm. The impedances of pure Cu and SS pipes are also plotted by blue and green dotted lines.

Longitudinal resistive-wall impedance of a two-layer round pipe was also derived as Eq. (4).

$$Z_{//}(\omega) = \frac{-i}{2\pi\varepsilon_0 bc\left\{\left(\frac{\omega}{\lambda_1 c}+\frac{\lambda_1 c}{\omega}\right)\alpha_{l2}-\frac{b\omega}{2c}\right\}} \qquad (4)$$

$$\alpha_{l2} = \frac{J_1(\lambda_1 b)+\kappa N_1(\lambda_1 b)}{J_0(\lambda_1 b)+\kappa N_0(\lambda_1 b)}$$

$$\lambda_{1,2} = \frac{i+sgn(\omega)}{\delta_{1,2}}, \quad \delta_{1,2} = \sqrt{\frac{2}{\sigma_{1,2}\mu_0|\omega|}}$$

$$\kappa = \frac{\left(\frac{\omega}{\lambda_1 c}+\frac{\lambda_1 c}{\omega}\right)H_0^{(1)}(\lambda_2(b+d))J_1(\lambda_1(b+d))-\left(\frac{\omega}{\lambda_2 c}+\frac{\lambda_2 c}{\omega}\right)H_1^{(1)}(\lambda_2(b+d))J_0(\lambda_1(b+d))}{\left(\frac{\omega}{\lambda_2 c}+\frac{\lambda_2 c}{\omega}\right)H_1^{(1)}(\lambda_2(b+d))N_0(\lambda_1(b+d))-\left(\frac{\omega}{\lambda_1 c}+\frac{\lambda_1 c}{\omega}\right)H_0^{(1)}(\lambda_2(b+d))N_1(\lambda_1(b+d))}$$

Here b, d, $\sigma_{1,2}$, $\delta_{1,2}$ are the inner radius of the pipe, the thickness of the inner layer, the electric conductivities and the skin depths of the inner and outer layers. The thickness of the outer layer is assumed to be infinite. Definitions of the other parameters are the same as those of the one-layer pipe in Eq. (1).

Figure 2 shows the real parts of the resistive-wall impedances of copper(Cu)-coated SS pipes with an inner radius of 8 mm and Cu-coating thicknesses of 1, 10 and 100 μm calculated from Eq. (4). The Cu coating corresponds to the inner layer of the two-layer pipe and the electric conductivity of Cu is 5.9×10^7 $\Omega^{-1}m^{-1}$. For comparison, the impedances of pure Cu and SS pipes with the same inner radius are shown in the same figure. As found in Fig. 2, the impedances of Cu-coated SS pipes agree with that of the pure SS pipe at low frequencies and the pure Cu pipe at high frequencies. The frequency where the transition from the SS to Cu impedance occurs depends on the Cu-coating thickness.

Transverse Impedance

An exact expression of the transverse resistive-wall impedance of a round pipe with an inner radius b and a thickness d was derived as

$$Z_{\perp}(\omega) = \frac{-i}{\pi\varepsilon_0 b^3\omega\left\{\left(\frac{2\omega}{\lambda c}+\frac{\lambda c}{\omega}\right)\alpha_t-\frac{b\omega}{2c}\right\}} \qquad (5)$$

$$\alpha_t = \frac{J_2(\lambda b)N_1(\lambda(b+d))-N_2(\lambda b)J_1(\lambda(b+d))}{J_1(\lambda b)N_1(\lambda(b+d))-N_1(\lambda b)J_1(\lambda(b+d))}$$

Parameter definitions are the same as described for Eq. (1). J_2 and N_2 are 2nd-order Bessel functions of the 1st and 2nd kinds, respectively. If the pipe thickness becomes infinity, the expression is rewritten as Eq. (6) with the 1st-order and 2nd-order Hankel functions of the 1st kind, $H_1^{(1)}$ and $H_2^{(1)}$.

$$Z_{\perp}(\omega) = \frac{-i}{\pi\varepsilon_0 b^3\omega\left\{\left(\frac{2\omega}{\lambda c}+\frac{\lambda c}{\omega}\right)\frac{H_2^{(1)}(\lambda b)}{H_1^{(1)}(\lambda b)}-\frac{b\omega}{2c}\right\}} \qquad (6)$$

The conventional expression is derived from Eq. (6) on the conditions of $|\lambda|b >> 1$, $|\lambda| >> |\omega/c|$, $|\lambda| >> b\omega^2/c^2$ as follows:

$$Z_{\perp}(\omega) = \frac{Z_0\delta}{2\pi b^3}\{sgn(\omega)-i\} \qquad (7)$$

Figure 3 shows the real parts of the transverse resistive-wall impedances of SS pipes with b=25 mm calculated from Eqs. (5) and (6). For comparison, the conventional expression of Eq. (7) is shown in the figure. The real parts of the transverse impedances also have low and high frequency cut-offs, each of which has a very similar dependency on pipe radius and thickness to that of the longitudinal one. It should be noted that, as the frequency decreases, the real parts of the exact resistive-wall impedances go down to zero, while that of the conventional expression continues to increase.

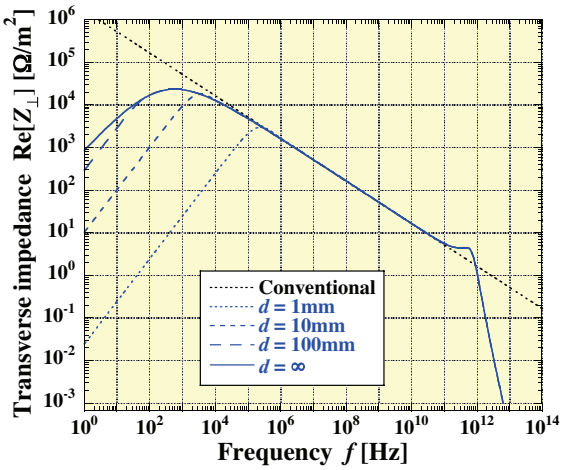

Figure 3: Transverse resistive-wall impedances of round pipes with an inner radius of 25 mm and thicknesses of 1, 10, 100 mm and infinity. The conventional impedance expression is also plotted by a black dotted line.

PARASITIC LOSS DUE TO LONGITUDINAL WAKEFIELDS

Loss Factor and Parasitic Loss

Loss factor of the resistive-wall pipe is expressed as Eq. (8) with the longitudinal impedance and the bunch length σ_t when the electron distribution of the bunch is Gaussian.

$$k = \frac{1}{\pi}\int_0^\infty Re\{Z_{//}(\omega)\}\exp\left\{-(\sigma_t\omega)^2\right\}d\omega \qquad (8)$$

If the bunch length becomes shorter, the high-frequency cut-off caused by the exponential term in Eq. (8) shifts to higher frequency and as a result the loss factor becomes higher. Since ERL-based SR sources have much shorter bunches than the storage-ring based SR sources, they have much higher loss factors.

Parasitic loss in a round pipe with the length L is expressed with the loss factor as

$$P_{RW} = kQ_b^2 f_b L = kI^2 L/f_b \qquad (9)$$

Here Q_b, f_b, and I are the bunch charge and the repetition frequency of bunches and the average beam current. The loss factor and parasitic loss per unit length in each of SS pipes with radii of 8 and 3 mm are calculated from Eqs. (8) and (9) for a typical ERL-based SR source (σ_t=1ps, I=100mA, f_b=1.3GHz):

k = 2.73(7.11) [V/pC/m] (b = 8(3)mm)

P_{RW}/L = 21.0(54.7) [W/m] (b = 8(3)mm)

The loss factor and the parasitic loss are also calculated for SPring-8 (σ_t=13ps, I=100mA, f_b=0.045GHz) as

k = 0.0562(0.150) [V/pC/m] (b = 8(3)mm)

P_{RW}/L = 13.3(35.3) [W/m] (b = 8(3)mm)

The typical ERL-based SR source has higher parasitic loss than SPring-8 (and than most of the existing 3rd generation SR sources) because of the higher loss factor.

Reduction of Parasitic Loss by Copper Coating

If a vacuum chamber is made of a very good electric conductor such as Cu for reducing the loss factor, eddy currents of the chamber can be considerable when the magnetic field of a magnet or insertion device is changed there. Cu coating is expected to reduce the loss factor of a SS vacuum chamber without significantly increasing effects of the eddy currents. As shown in Fig. 2, only 1-μm Cu coating can suppress the dominant high frequency component in the longitudinal impedance of the SS pipe. The loss factor and parasitic loss of the Cu-coated pipe are numerically calculated from Eqs. (8) and (9) as

k = 0.404(1.07) [V/pC/m] (b = 8(3)mm)

P_{RW}/L = 3.11(8.26) [W/m] (b = 8(3)mm)

The obtained parasitic loss is about one seventh of that of the pure SS pipe and equal to that of the pure Cu pipe. This calculation result confirms the effectiveness of Cu coating in reducing the parasitic loss of a SS vacuum chamber.

BEAM BREAKUP DUE TO TRANSVERSE WAKEFIELDS

Wake Function

The transverse wake function is expressed with the transverse impedance as in Eq. (10).

$$\begin{aligned} W_\perp(t) &= \frac{-i}{2\pi}\int_{-\infty}^{\infty} Z_\perp(\omega)e^{-i\omega t}d\omega \\ &= -\frac{2}{\pi}\int_{-\infty}^{\infty} Re\{Z_\perp(\omega)\}\sin(\omega t)d\omega \end{aligned} \qquad (10)$$

If Eq. (7) is used in Eq. (10) as the impedance, the conventional expression for the transverse wake function of a round pipe is obtained as Eq. (11), which is valid only for the condition of (12).

$$W_\perp(t) = -\frac{1}{\pi b^3 t^{1/2}}\sqrt{\frac{cZ_0}{\pi\sigma}} \qquad (11)$$

$$2\pi\sqrt[3]{b^2/\sigma Z_0}\,/c << t << 2\pi\mu_0\sigma b^2, t << 2\pi\mu_0\sigma d^2 \qquad (12)$$

Exact wake functions were numerically calculated from Eqs. (5) and (10). Red solid lines in Figs. 2(a) and 2(b) show the calculated exact wake functions for two different SS pipes with inner radii of 25-mm and 3-mm radius and a thickness of 1 mm. A black dotted line and a blue solid line in each figure show the conventional wake function of Eq. (11) and the ratio of the exact to the conventional wake function, respectively. As clearly shown by the ratio of the exact to the conventional wake function, each exact wake function more quickly and substantially decreases compared with the conventional wake function.

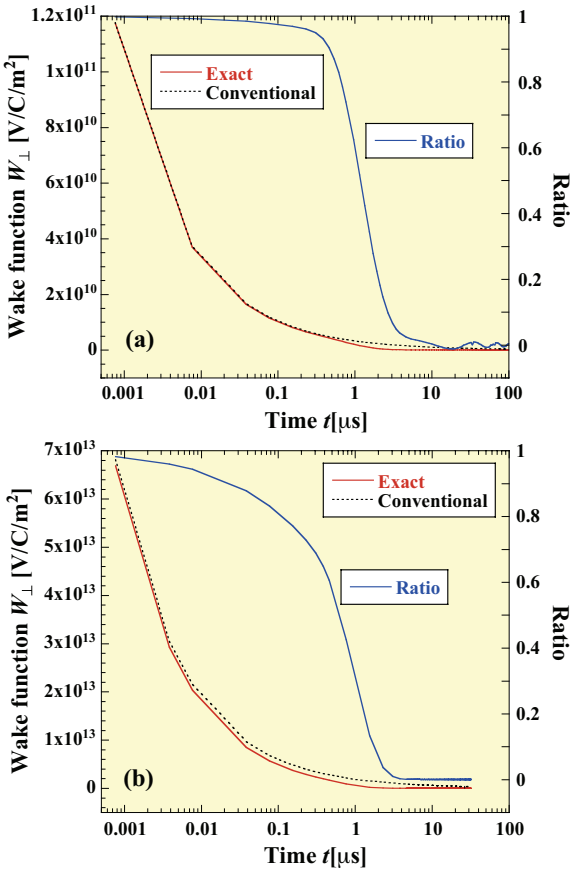

Figure 4: Exact transverse wake functions of two different SS pipes (red solid lines): (a) b=25mm and d=1mm and (b) b=3mm and d=1mm. black dotted and blue solid lines indicate the conventional expression and ratio of the exact to the conventional wake function, respectively.

Equation of Motion

The equation of transverse motion for the M-th electron bunch injected into an ERL under the resistive-wall wake is as follows:

$$y_M''(s) + K(s)y_M(s) = 0 \quad (M = 1) \tag{13}$$

$$y_M''(s) + K(s)y_M(s) = \sum_{N=1}^{M-1} h(M-N)y_N(s) \quad (M \geq 2) \tag{14}$$

$$h(M) = \frac{eI\tau_B}{E} W_\perp(M\tau_B), \quad I = \frac{eN_B}{\tau_B} \tag{15}$$

Here K, e, N_B, E and τ_B are the external focusing, the electron charge, the electron number per bunch, the electron energy and the time separation between bunches. The right-hand term of Eq. (14) means a transverse kick due to the resistive-wall wake. Since the bunch number M can be replaced with t/τ_B for $M >> 1$, the transverse position y_M of the M-th bunch is represented as a function of the time t and the longitudinal position s:

$$y_M(s) \rightarrow y(t,s),\ t \cong M\tau_B \left(M >> 1\right)$$

Hereafter $y(t,s)$ or y is used as the transverse beam position in place of y_M.

Resistive-Wall BBU Simulation

Based on Eqs. (13) to (15), resistive-wall BBU simulations in the compact ERL[3] were performed. Figure 5 shows layout of the compact ERL and the simulation path. The simulation start and end points are just after the acceleration and just before the deceleration due to accelerating cavities in the two superconducting (SC) cryomodules as shown in Fig. 5. The path length L between the two points is 55.44 m. In the simulations, effects of the magnet fields were not considered. The electron beam was assumed to have an energy of 60 MeV, a repetition rate of 1.3 GHz and an average beam current of 100 mA (a bunch charge of 77pC). All the bunches were injected with an initial position offset y_0 at the simulation start point. The transverse beam position y can always be normalized by y_0.

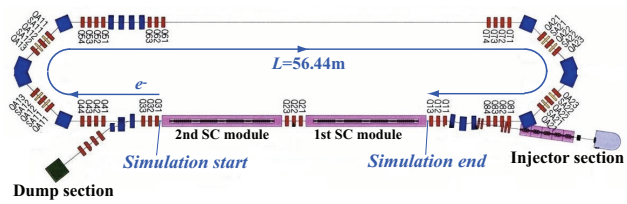

Figure 5: Layout of the compact ERL and the simulation path.

First the vacuum duct of the compact ERL was assumed to be a round SS pipe with b=25mm and d=1mm. The 25-mm radius is standard for the compact ERL vacuum ducts. Figure 6(a) shows the simulation result of the transverse beam motion for this SS pipe. The transverse beam position y at the simulation end point is increased with time and then saturated to 2 % of y_0 in a short time. In this case, effects of the resistive-wall wake are not serious. On the other hand, when the conventional wake function is used in the simulation, the transverse position is not saturated and increased infinitely with time. But this is not true. It is essential to use the exact wake function for correctly studying the resistive-wall BBU. Next the vacuum duct was assumed to be a round SS pipe with b=3 mm and d=1 mm. Figure 6(b) shows the simulation result. Although the transverse beam position is also saturated, it is increased up to 28 times of y_0. In this case, the beam hits the pipe when the initial position offset is larger than 110 μm, and the resistive-wall BBU can easily occur. Generally, when the beam energy is low and the pipe is very narrow and long, the resistive BBU becomes serious.

Finally transverse beam motion was simulated in a long undulator vacuum chamber (b=3 mm, d=1 mm) of a 5-GeV ERL SR source with a repetition rate of 1.3 GHz and an average beam current of 100 mA. The length of the undulator vacuum chamber was considered up to 100 m. Effects of magnetic field of the undulator was not considered. Figures 7(a) and 7(b) show the simulated transverse beam position at the exit of the 100-m chamber as a function of time and the dependence of the saturated position on the chamber length (at t=32.3 μs). Since the

beam energy is high, the transverse beam position is saturated to about 30 % of y_0 even for the chamber length of 100 m. The beam position displacement becomes smaller when the chamber length is shorter as shown in Fig. 7(b). However the assumed 1-mm thickness of the chamber is thinner than the ordinary one and the effective thickness including the surroundings such as undulator itself may have to be considered. Thus it is practically necessary to simulate transverse beam motions in thicker chambers

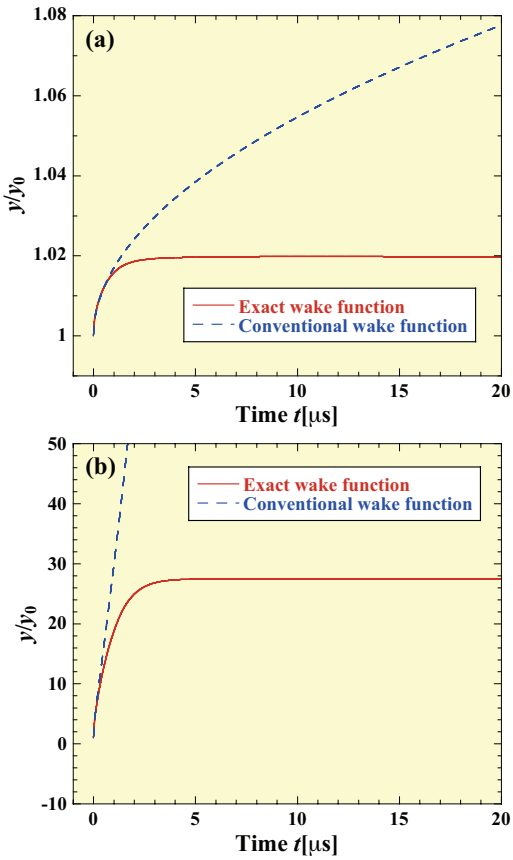

Figure 6: Simulated transverse beam position y normalized by y_0 in the compact ERL for SS pipes: (a) b=25mm and d=1mm and (b) b=3mm and d=1mm. Blue broken lines indicate simulation results using the conventional wake function.

SUMMARY

Exact expressions of longitudinal and transverse resistive-wall impedances of round pipes were obtained in order to correctly study effects of the resistive-wall wakefields. It was shown by calculations using the longitudinal impedance expressions that the parasitic loss of an ERL-based SR source can be higher than those of 3rd generation SR sources and at the same time that Cu coating can effectively reduce the impedance of a SS vacuum chamber. Based on the exact wake functions calculated from the transverse impedance expression, transverse beam motion was simulated for the compact ERL and an undulator chamber of a 5-GeV ERL and as a result it was found that the transverse beam position displacement due to the resistive-wall wakefields is saturated in a short time and does not continue to increase infinitely. The maximum position displacements in the compact ERL are 0.02 and 28 times of the initial position offset for the 1-mm thick SS vacuum pipes with 25 and 3 mm radii, respectively. The resistive-wall BBU is serious in the latter case and not in the former case. In the SS undulator chamber with 3-mm radius and 1-mm thickness of the 5-GeV ERL, the maximum position displacement was 30 % of the initial position offset even for 100-m chamber length because of the higher energy. Further simulations in thicker vacuum chambers are needed for more practical situations.

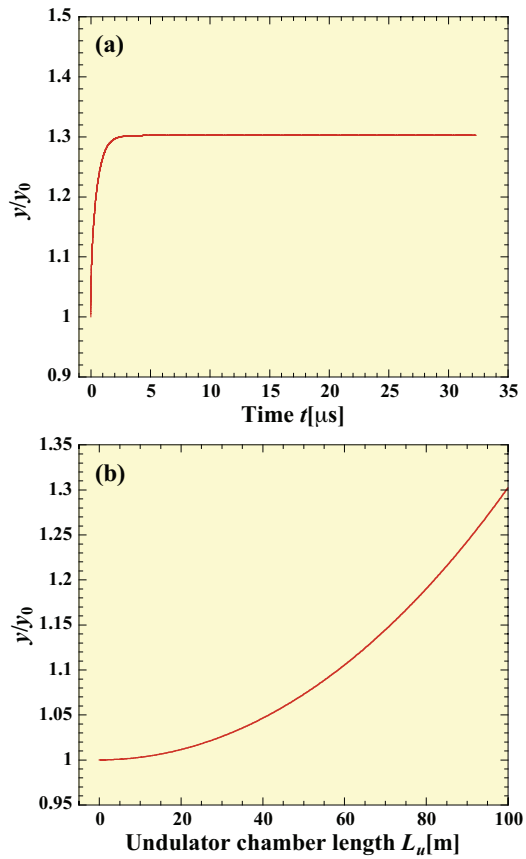

Figure 7: Simulated transverse beam position y normalized by y_0 in an undulator SS vacuum chamber: (a) dependence on time at L_u=100 m and (b) dependence on chamber length at t=32.6 μs.

REFERENCES

[1] J. M. Wang and J. Wu, Phys. Rev. ST Accel. Beams **7**, 034402(2004).

[2] N. Nakamura, Proceedings of ERL07, Daresbury Laboratory, May 21-25, pp45-49(2007).

[3] R. Hajima, N. Nakamura, S. Sakanaka, Y. Kobayashi (eds.), KEK Report 2007-7/JAEA-Research 2008-032.